

筑 波 大 学

博 士 （ 医 学 ） 学 位 論 文

MicroRNA-205-5p suppresses invasiveness in oral
squamous cell carcinoma by inhibiting TIMP-2 expression

(MicroRNA-205-5p は TIMP-2 の発現抑制を介し
て口腔扁平上皮癌の浸潤能を抑制する)

2 0 1 7

筑波大学大学院博士課程人間総合科学研究科

長 井 宏 樹

目次

Introduction (背景)	• • • • • 1
--------------------------	-------------

Purpose (目的)	• • • • • 2
---------------------	-------------

Material and methods (方法と対象)	• • • • • 2
-------------------------------------	-------------

- *OSCC clinical specimens and cell lines*
- *TaqMan-based quantitative qRT-PCR assay of miRNA expression*
- *TaqMan-based qRT-PCR assay of mRNA expression*
- *Transfection with miR-205-5p mimic or inhibitor or with siRNA*
- *Cell proliferation, migration, and invasion assay*
- *Identification of candidate genes regulated by miR-205-5p*
- *Dual-luciferase reporter assay*
- *Western blotting*
- *Gelatin zymography*
- *MMP-2 activity assay*
- *Statistical analysis*

Result (結果)	• • • • • 8
--------------------	-------------

- *MiR-205-5p in OSCC cell lines and clinical specimens*

- *Effect of miR-205-5p mimic or inhibitor on cell proliferation, migration, and invasion*
- *Identification of miR-205-5p target gene in OSCC*
- *TIMP-2 is a direct target of miR-205-5p in OSCC*
- *Effect of TIMP-2 silencing in OSCC cell lines*
- *Suppression of TIMP-2 reduces the activation of pro-MMP2 by TIMP-2/MT1-MMP complex*

Discussion (考察)	• • • • • 11
Table and Figure (表と図)	• • • • • 16
References (参考文献)	• • • • • 25

参考論文

Introduction

Oral squamous cell carcinoma (OSCC) represents more than 95% of oral-cavity cancer(1). In developing countries, OSCC is the sixth most common cancer. OSCC has an overall 5-year survival rate of less than 50%(1), and this poor prognosis is due mainly to a high likelihood of metastasis to lymph nodes in the neck(2-5). Despite recent advances in treatment modalities such as surgery, radiotherapy, and chemotherapy, the survival rates for OSCC have not markedly improved(6). Thus, metastasis to neck lymph no prognostic des is a major factor in OSCC.

Tumor invasion and metastasis require tumor cells to resolve and move through the extracellular matrix (ECM). Matrix metalloproteinases (MMPs) and tissue inhibitors of metalloproteinases (TIMPs) are important for degrading the ECM during these processes(7). Matrix metalloproteinase-2 (MMP-2) is especially important in tumor-cell invasion because it can deconstruct collagen type IV, the major constituent of basement membranes(8). The proteolytic activation of MMP-2 is controlled by TIMP-2, which is necessary for activating pro-MMP-2(9, 10). TIMP-2 forms a complex with membrane type-I metalloproteinase 1 (MT1-MMP) on cell membranes, and the TIMP-2/MT1-MMP complex activates pro-MMP-2. Thus, an imbalance in MMP-2 and TIMP-2 might disrupt the balance of ECM turnover and lead to uncontrolled degradation of the ECM, including basement membranes, and is the most likely cause of tumor invasion and metastasis(7). Thus, it may be possible to control pro-MMP-2 activation, and therefore tumor invasion and metastasis, by regulating TIMP-2.

MicroRNAs (miRNAs), which are short, non-coding RNAs of 20–22

nucleotides, regulate gene expression at the post-transcriptional level by interacting with the 3'-untranslated regions (3'-UTR) of the target gene(11). MiRNAs are involved in a wide range of biological functions, and can function as oncogenes or tumor suppressors according to the functions of the target genes. To date, several miRNAs have been implicated in the progression of OSCC, including miR-26a/b, miR-23b/27b, miR-155, miR-221, and miR-205(12-16). Recent studies show that miR-205-5p is downregulated in various cancer cells, including breast cancer, prostate cancer, and oral cancer(17-19). In addition, the transient overexpression of miR-205-5p in cancer cells is reported to suppress tumor progression by inhibiting tumor-associated genes and upregulating tumor-suppressing genes. However, the signaling pathway and anti-tumorigenic functions of miR-205-5p in various cancer cells are unclear.

Purpose

The present study was conducted to determine the function of miR-205-5p in OSCC and the molecular mechanism by which miR-205-5p suppresses OSCC tumor progression.

Material and Methods

OSCC clinical specimens and cell lines.

OSCC cell lines (HSC3 and SAS) obtained from the Japanese Collection of Research Bioresources (Osaka, Japan) were cultured as previously described(14). We authenticated HSC3 and SAS through short tandem repeat (STR) profiling (PowerPlex 16 STR System) in 2017 and ensure that no culture contamination occurred. We

obtained 71 primary OSCC tissue, and 28 lymph node metastases tissue from 71 previously untreated subjects with OSCC who visited the University of Tsukuba Hospital between February 2008 and November 2010, and from 6 subjects who did not have cancer. Primary and metastatic specimens were collected at the time of biopsy and neck dissection respectively. And they prepared for formalin-fixed paraffin-embedded (FFPE) histology using standard procedures. OSCC was diagnosed and classified based on the Tumor-Node Metastasis (TNM) system of Unio Internationalis Contra Cancrum (UICC). All OSCC cases were diagnosed clinically and confirmed histologically by pathologists. The clinical characteristics of the OSCC patients are shown in Table I.

This study was reviewed and approved by the Ethics Committee University of Tsukuba Hospital (No. 215). All patients gave informed written consent prior to enrollment.

TaqMan-based quantitative (q) RT-PCR assays of miRNA expression.

Total RNA was extracted with the miRNeasy Mini Kit (Qiagen, Venlo, Limburg, Netherlands) for cell lines and the miRNeasy FFPE Kit (Qiagen) for FFPE. Reverse transcription was performed using the TaqMan MicroRNA Reverse Transcription Kit (Applied Biosystems, Foster City, CA, USA). MiR-205 expression was measured using the TaqMan MicroRNA Assay system (Applied Biosystems) according to the manufacturer's instructions. PCR reactions were performed using the CFX384 Real-Time System (Bio-Rad Laboratories, Pleasanton, CA, USA). The small RNA RNU6B was used as internal control. Relative expression was calculated by the

comparative threshold (Ct) method.

TaqMan-based qRT-PCR assay of mRNA expression.

Total RNA was extracted with the RNeasy Mini Kit (Qiagen) and reverse-transcribed with the PrimeScript RT Reagent Kit (TaKaRa, Shiga, Japan). PCR reactions were conducted using the CFX384 Real-Time System (Bio-Rad Laboratories). Relative mRNA expression was normalized against GAPDH. Relative expression was calculated by the comparative threshold (Ct) method. The following qRT-PCR primers were used: for TIMP-2, 5'-GCCCCCGCCCGCCCAGCCCCC-3' (forward) and 5'-GCAACAATATCCACTTTACCAGAGTTAA-3' (reverse); for GAPDH, 5'-CAACGGATTTGGTCGTATTGG-3' (forward) and 5'-GCAACAATATCCACTTTACCAGAGTTAA-3' (reverse).

Transfection with miR-205-5p mimic or inhibitor or with siRNA.

Cells were cultured to 70–80% confluence in 12-well plates and transfected with 50 nM miR-205-5p mimic or inhibitor (hsa-miR-205 *mirVana*TM miRNA Mimic, #4464066; *mirVana*TM miRNA Inhibitor, #4464084), or with 50 nM scramble negative control (*mirVana*TM miRNA Mimic Negative Control, #4464058; *mirVana*TM miRNA Inhibitor Negative Control, #4464076) from Ambion (Austin, TX, USA). To knock down TIMP-2, cells were transfected with 25 nM TIMP-2 siRNA (Silencer®Select siRNA, #4390824) or control siRNA (Silencer®Negative control siRNA, #AM4611). Lipofectamine RNAiMAX transfection reagent (Invitrogen, Carlsbad, CA, USA) was used according to the manufacturer's instructions. The cells were incubated for 24 h

after transfection, the medium was exchanged for FBS-free medium, and the cells were incubated for another 48 h. Both the transfected cells and the culture media were used for assays and analyses, as described below.

Cell proliferation, migration, and invasion assays.

Cells were cultured as described previously(14). Cell proliferation was performed as described in previous study. Cells were transfected with 50nM miR-205-5p mimic or inhibitor by reverse transfection and plated in 96 well plates at 3×10^3 cells per well. After 72h, cell proliferation was determined with the MTT assay using MTT Cell Count Kit (Nakalai Tesque, Kyoto, Japan). Cell migration was measured with the 96-well BME Cell-Invasion Assay according to the manufacturer's instructions (Trevigen, Inc., MD, USA). Invasiveness was assayed by the three-dimensional Matrigel culture method(20, 21): 8×10^5 transfected cells were suspended in 200 μ L Matrigel (Corning, NY, USA). A 150- μ L drop of Matrigel mixture containing transfected cells was polymerized on the bottom of a 6-well microplate and incubated in 2 mL medium for 48 h. Photographs were taken by fixed-point observation at 40 \times magnification under a BZ-X700 microscope (Keyence, Osaka, Japan). Invasiveness was assessed by the distance of cell migration. The distance of cell migration represented the length from the gel surface to the migratory front of cells invaded out of gel.

Identification of candidate genes regulated by miR-205-5p.

Possible miR-205-5p targets were identified by bioinformatics analysis with

the TargetScan algorithm and integrated analysis across data for human cancer-cell lines and mRNA microarray data to identify miRNAs whose expression was correlated with the inverse expression of the mRNA targets predicted *in silico*.

Plasmid construction and dual-luciferase reporter assay

Partial wild-type sequences of the TIMP-2 3'-UTR or those with a deleted miR-205-5p target sites (positions 590-596 of the TIMP-2 3'-UTR) were inserted between the XhoI-PmeI restriction sites in the 3'-UTR of hRluc gene in the psiCHECK-2 vector (Promega, Madison, WI, USA). The protocol for vector construction was as described previously (22, 23). The synthesized DNA was cloned into the psiCHECK-2 vector. HSC3 cells were transfected with 50 ng of the vector and 50nM miR-205-5p mimic using Lipofectamine 3000 (Invitrogen, Carlsbad, CA, USA). The activities of firefly and Renilla luciferases in cell lysates were determined with a Dual-luciferase Reporter assay system (Promega). Normalized data were calculated as the ratio Renilla/firefly luciferase activities.

Western blotting.

Cells were incubated for 72 h after transfection, and then cell lysates were prepared. In addition, the culture media were centrifuged and the supernatants were collected. The supernatants were inspissated with a Vivaspins 2-10K (GE Healthcare UK Ltd, Little Chalfont, UK) according to the manufacturer's instructions. Next, 15 µg of protein lysates were separated on Mini-PROTEIN TGX Gels (Bio-Rad, Hercules, CA, USA) and transferred to Trans-Blot Turbo Mini PVDF membranes (Bio-Rad,

Hercules, CA, USA). The membranes were probed with rabbit anti-TIMP-2 antibodies (1:1000; #5738; Cell Signaling Technology, Danvers, MA, USA), rabbit MT1-MMP antibodies (1:1000; ab51074; Abcam, Cambridge, UK), and goat anti-actin antibodies (1:1000; sc1615; Santa Cruz Biotechnology, Texas, USA) overnight at 4°C. Proteins were detected with Chemi-Lumi One Super (Nakalai Tesque, Kyoto, Japan), and images of the blots were obtained with a ChemiDoc XRS Plus system (Bio-Rad, Hercules, CA, USA).

Gelatin zymography.

MMP-2 enzyme activity was analyzed in cell supernatants by gelatin zymography using the Gelatin Zymography Kit (Cosmo Bio Co., Ltd; Tokyo, Japan) according to the manufacturer's instructions. Images were obtained using the ChemiDoc XRS Plus system (Bio-Rad, Hercules, CA, USA).

MMP-2 activity assay.

The enzymatic activated MMP-2 content and total MMP-2 in cell supernatants were determined using the QuickZyme Human MMP-2 Activity Assay (QuickZyme BioSciences, Leiden, Netherlands) according to the manufacturer's instructions.

Statistical analysis.

Data for *in vitro* experiments were evaluated by the Student's *t*-test. Relationships among more than three variables and numerical values were analyzed using Kruskal-Wallis test with Steel-Dwass test. The analysis of disease-specific

survival was performed by the Kaplan-Meier method and compared using the Log-rank test. Correlations between miR-205-5p and TIMP-2 expression were evaluated by Spearman's rank test. All statistical analyses were performed using JMP version 11.

Results

MiR-205-5p in OSCC cell lines and clinical specimens.

I evaluated the miR-205-5p expression in 71 primary OSCC specimens, 28 metastatic OSCC specimens (Table I), and in the HSC3 and SAS cell lines. And I found that the miR-205-5p expression was significantly lower in primary OSCC tissue than in normal oral mucosa adjacent to the biopsied tumor tissue, and that the expression was even lower in metastatic OSCC tissue than in primary OSCC tissue (Fig. 1A). On the other hand, the miR-205-5p expression was relatively low in primary OSCC tissue with metastasis compared to that without metastasis ($p=0.103$). Further, I determined the cut-off value ($=3.74$) of miR-205-5p in primary OSCC tissue by receiver operating characteristic (ROC) curve and analyzed disease specific survival by the Kaplan-Meier method and compared using the Log-rank test. There was no difference between miR-205-5p high expression group and miR-205-5p low expression group (Fig. 1B).

Effect of miR-205-5p mimic or inhibitor on cell proliferation, migration, and invasion.

Proliferation was not suppressed in HSC3 or SAS cells transfected with miR-205-5p mimic compared to the negative control (Fig. 2A). HSC3-cell migration

was significantly suppressed by transfection with miR-205-5p mimic compared to the negative control, but SAS-cell migration was not (Fig. 2B). Invasiveness was significantly suppressed in both HSC3 and SAS cells transfected with miR-205-5p mimic compared to the negative control (Fig. 2C). The number of cells invaded out of gel was almost proportional to the migration distance. On the other hand, proliferation had no difference in HSC3 and SAS cells transfected with miR-205-5p inhibitor compared to the negative control (Fig. 2D). Both migration and invasiveness were significantly enhanced in HSC3 and SAS cells transfected with miR-205-5p inhibitor as compared to negative control (Fig. 2E, F).

Identification of miR-205-5p target genes in OSCC.

I screened the TargetScan database for possible target genes containing a putative miR-205-5p-binding site in their 3' UTR, and identified 5974 candidate genes that might be regulated by miR-205-5p. From these, I selected genes related to TIMPs and MMPs, and identified three candidate miR-205-5p targets (Table II). Among these candidates, I focused on the TIMP-2 gene, because Spearman's rank test showed a significant negative correlation between the expression of TIMP-2 mRNA and that of miR-205-5p in OSCC specimens (Fig. 3A-C)

TIMP-2 is a direct target of miR-205-5p in OSCC cells.

The TargetScan database showed one putative, poorly conserved miR-205-5p-binding site in the 3'-UTR of TIMP-2 (position 590–596) (Fig. 4A). I investigated the TIMP-2 expression in miR-205-5p mimic-transfected OSCC cells,

and found that the TIMP-2 mRNA and protein were suppressed in cells transfected with miR-205-5p mimic compared to the negative control (Fig. 4B, C). To determine whether the TIMP-2 mRNA contains a target site for miR-205-5p, I conducted luciferase reporter assays in HSC3 and SAS cells. The TargetScan database showed that there was one putative miR-205-5p binding site in the TIMP-2 3'-UTR (position 590-596). I used vectors encoding either a partial wild-type sequence (including the predicted miR-205-5p target site) or deletion of the seed sequence of the 3'-UTR of TIMP-2 mRNA. I found that the luciferase activity was significantly suppressed by cotransfection with miR-205-5p mimic and the vector carrying the wild-type 3'-UTR of TIMP-2 (Fig. 4D).

Effect of TIMP-2 silencing in OSCC cell lines.

I next investigated TIMP-2's function in HSC3 and SAS cells by loss-of-function studies using si-TIMP-2 transfection. Western blots and qRT-PCR indicated that si-TIMP-2 effectively downregulated the TIMP-2 expression in both cell lines (Fig. 5A, B). Invasiveness was suppressed in both HSC3 and SAS cells when transfected with si-TIMP-2 compared to the negative control (Fig. 5C).

Suppression of TIMP-2 reduces the activation of pro-MMP2 by the TIMP-2/MT1-MMP complex.

To investigate whether reducing TIMP-2 expression could affect the activation of pro-MMP2 by MT1-MMP, I used western blots or gelatin zymography to measure the expression of TIMP-2, MT1-MMP, pro-MMP2, and active-MMP2 in HSC3 and

SAS cells transfected with miR-205-5p mimic or si-TIMP-2. Western blots showed that the TIMP-2 expression was reduced in the supernatant of both cells transfected with miR-205-5p mimic or si-TIMP-2 compared to the negative control, and that the MT1-MMP expression was comparable in both cells transfected with miR-205-5p mimic, si-TIMP-2, or negative control (Fig. 6A). Next, I measured the pro-MMP2 activation in cell supernatants (see Material and Methods). The MMP-2 activity assay showed that the rate of pro-MMP-2 activation was significantly lower in both cells transfected with miR-205 mimic or si-TIMP-2 than in those transfected with the negative control (Fig. 6B). The rate of pro-MMP-2 activation represented the percentage of active-MMP-2 to total MMP-2 (pro-MMP-2 + active-MMP-2). The gelatin zymography showed that activated pro-MMP-2 (active-MMP-2) was decreased in both cells transfected with miR-205-5p mimic than in those transfected with the negative control (Fig. 6C).

Discussion

There is growing evidence for the involvement of miRNAs in several biological processes, including human oncogenesis and metastasis(24); these include miR-29c, miR-335, and miR-375(25, 26). Studies show that miR-155-5p is downregulated in OSCC tissue, and that a low miR-155-5p level is correlated with a poor prognosis(14). Therefore, the investigation of miRNA-expression signatures in cancer specimens is an important research avenue. My present study, which focused on miR-205-5p, produced three major findings: first, that miR-205-5p was tumor-suppressive in OSCC

cells (Fig. 1 and 2); second, that miR-205-5p directly suppressed TIMP-2 expression in OSCC cells (Fig. 4); and third, that by suppressing TIMP-2 expression, miR-205-5p inhibited pro-MMP-2 activation (Fig. 6).

In this study, I observed that the miR-205-5p expression was significantly downregulated in OSCC tissues and cell lines compared to normal oral mucosa adjacent to the biopsied OSCC tissue (Fig. 1A). I also showed that transfection with miR-205-5p suppressed the invasiveness of both HSC3 and SAS cells (Fig. 2C). These results suggested that miR-205-5p acts as a tumor-suppressive miRNA in OSCC, and that reduced miR-205-5p expression may significantly contribute to OSCC invasion and metastasis. Recent studies show that miR-205-5p is downregulated in several types of cancer, including breast, prostate, and bladder cancer(27-29), and that miR-205-5p suppresses several tumor types by targeting oncogenes(16, 19, 30-32). Other studies show that miR-205-5p suppresses cell invasiveness in several types of cancer(33). The role of miR-205-5p in suppressing cell invasion has also been confirmed in *in vivo* models of breast cancer(28). These findings are consistent with my present results. In contrast, Kaplan–Meier analysis showed that there was no difference between miR-205-5p high expression group and miR-205-5p low expression group (Fig. 1B). Recent study shows that low expression of miR-205 was associated with poor prognosis in cervical cancer (34). Other recent study shows that low expression of both miR-205 and let-7d was associated with poor prognosis in HNSCC, but low expression of only miR-205 was not associated (35). To reveal the relation between expression of miR-205-5p and disease specific survival in OSCC, it will be necessary to research more OSCC cases.

One miRNA can regulate several protein-coding genes. Indeed, bioinformatic studies show that at least 30–60% of the protein-coding genes in the human genome are regulated by miRNAs(36). Therefore, a reduced expression of tumor-suppressive miRNAs may cause an overexpression of oncogenic genes in cancer cells.

In this study, I identified TIMP-2 as a miR-205-5p target. Other recent studies show that TIMP-2 is an oncogenic factor in several types of cancer. My data showed a significant negative correlation between the expression of TIMP-2 mRNA and that of miR-205-5p in OSCC tissues ($R = -0.318$, $p = 0.0074$) (Fig. 3). Furthermore, my luciferase reporter assays confirmed that miR-205-5p miRNA directly binds the 3'-UTR of TIMP-2 (Fig. 4D). This is the first report to show that TIMP-2 is directly regulated by miR-205-5p in OSCC cells.

TIMP-2 is known to regulate MMP through its enzymatic activity. My present data showed that silencing TIMP-2 suppressed invasiveness in OSCC cells (Fig. 5), suggesting that TIMP-2 promotes OSCC tumor progression. Recent immunohistochemical analyses identified elevated TIMP-2 as an indicator of aggressive behavior and a poor prognosis in patients with HNSCC(37), and demonstrated a strong correlation between marked TIMP-2 expression and lymph-node metastasis, as well as a poor prognosis, in the early stages of OSCC(37-39). These reports are consistent with my findings indicating that TIMP-2 may promote OSCC tumor progression. Recent studies show that TIMP-2 promotes tumor progression by the activation of MMP-2, which is mediated by MT1-MMP(9, 10). TIMP-2 was long thought to suppress tumor invasion by inhibiting MMP-2 in general, and when overexpressed, TIMP-2 inhibited MMP-2 *in vitro*. However,

according to a model of cell-mediated MMP-2 activation, pro-MMP-2 binds TIMP-2 in a complex with MT1-MMP on the cell surface, forming a pro-MMP-2/TIMP-2/MT1-MMP ternary complex. In this case, the pro-MMP-2 is activated by the adjacent MT1-MMP that is not bound to TIMP-2(9, 10, 40). In my present study, although I observed that TIMP-2 was reduced in the supernatant of miR-205-5p mimic-transfected HSC3 and SAS cells, the MT1-MMP expression was unchanged (Fig. 6A). In addition, pro-MMP-2 was activated at a lower rate in miR-205-5p mimic-transfected both cells (Fig. 6B, C). These results suggest that miR-205-5p suppresses the pro-MMP-2 activation by regulating TIMP-2, as illustrated in Figure 7. Recent studies show that TIMP-2 enhances the pro-MMP-2 activation via MT1-MMP *in vivo*(41-45), and that upregulating TIMP-2 promotes MMP-2 activation and the invasiveness of glioma cells(43). Another study showed that the ratio of MMP-2 activation is strongly correlated with TIMP-2 expression in SCC of the tongue(38). These findings are consistent with my present results. Pro-MMP-2 activation depends on the local TIMP-2 concentration; this activation and occurs at a low concentration of TIMP-2 relative to MT1-MMP, leaving sufficient inhibitor-free MT1-MMP to initiate the activation of pro-MMP-2(46, 47). On the other hand, high TIMP-2 levels inhibit MMP-2 activation by blocking all of the available MT1-MMP molecules (48). In my present study, the amount of TIMP-2 secreted into the culture medium appeared to be appropriate for regulating the MMP-2 activation in HSC3 and SAS cells. To further determine the role of miR-205-5p's regulation of TIMP-2 in OSCC, it will be necessary to use animal models.

In summary, the present study demonstrated that miR-205-5p functions as a

tumor suppressor in OSCC, that miR-205-5p directly regulates TIMP-2 expression, and that miR-205-5p suppresses pro-MMP-2's activation by regulating the TIMP-2 expression in OSCC cells (Fig. 7).

This identification of the tumor-suppressive role of miR-205-5p in OSCC may have significant therapeutic potential. Currently, RNA interference is being implemented as a gene-specific approach in molecular medicine. Thus, it may be possible to use miR-205-5p to regulate specific tumor-progressive genes as a novel therapeutic approach to treating OSCC.

Acknowledgments

This is a post-peer-review, pre-copyedit version of an article published in International Journal of Oncology. The final authenticated version is available online at <https://doi.org/10.3892/ijo.2018.4260>.

Tables

Table I. Clinical classification of OSCC patients

	Primary OSCC			Metastatic OSCC
	Total	Lymph node Negative (n = 41)	Lymph node Positive (n = 30)	Metastatic lymph node (n = 28)
Age				
< 60	18	7	11	9
≥ 60	53	34	19	19
Gender				
Male	47	24	23	21
Fema	24	17	7	7
Primary				
Tong	33	20	13	12
Gum	23	15	8	7
Bucc	7	4	3	3
Other	8	2	6	6
pTNM				
I - II	28	28	0	0
III-IV	43	13	30	28

pTNM: Pathological tumor node metastasis

Table II. miR-205-5p candidate target genes				
Gene symbol	Representative transcript	Gene name	Conserved	Poorly conserved
TIMP-2	NM_003255	Metallopeptidase inhibitor 2	0	1
MMP16	NM_005941	Matrix metallo-peptidase 16	0	1
MMP19	NM_002429	Matrix metallo-peptidase 19	0	1

Figure

Figure. 1

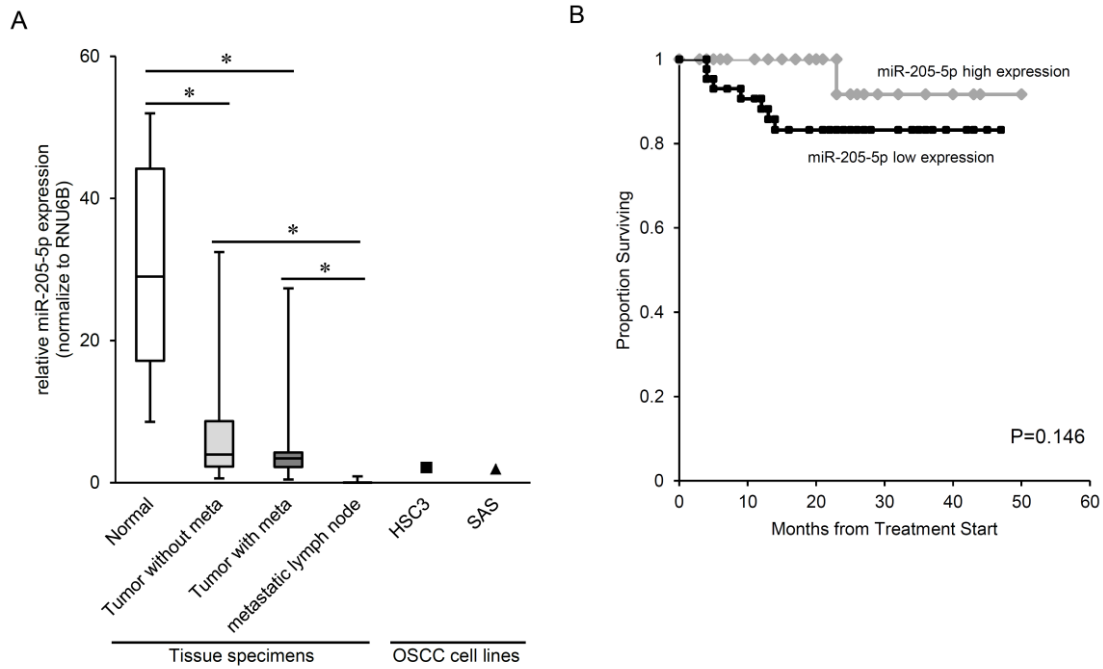


Figure 1. miR-205-5p expression in OSCC cell lines and clinical specimens. (A) Clinical specimens were classified as tissue with normal epithelia (n = 6), primary tumor tissue without lymph-node metastasis (n = 41), primary tumor tissue with lymph-node metastasis (n = 30), or metastatic tumor tissue (n = 28). The HSC3 and SAS cell lines were used to analyze miRNA expression and function. RNU6B was used for normalization. Box-and-whisker plots represent data from clinical specimens. Middle line, median; lower whisker, minimum; upper whisker, maximum. Shapes representing cell lines show the median. (*P < 0.05) (B) Kaplan-Meier curves for overall survival in 29 subjects with miR-205-5p high expression and 42 subjects with miR-205-5p low expression. The difference between these two groups is determined by the long-rank test.

Figure. 2

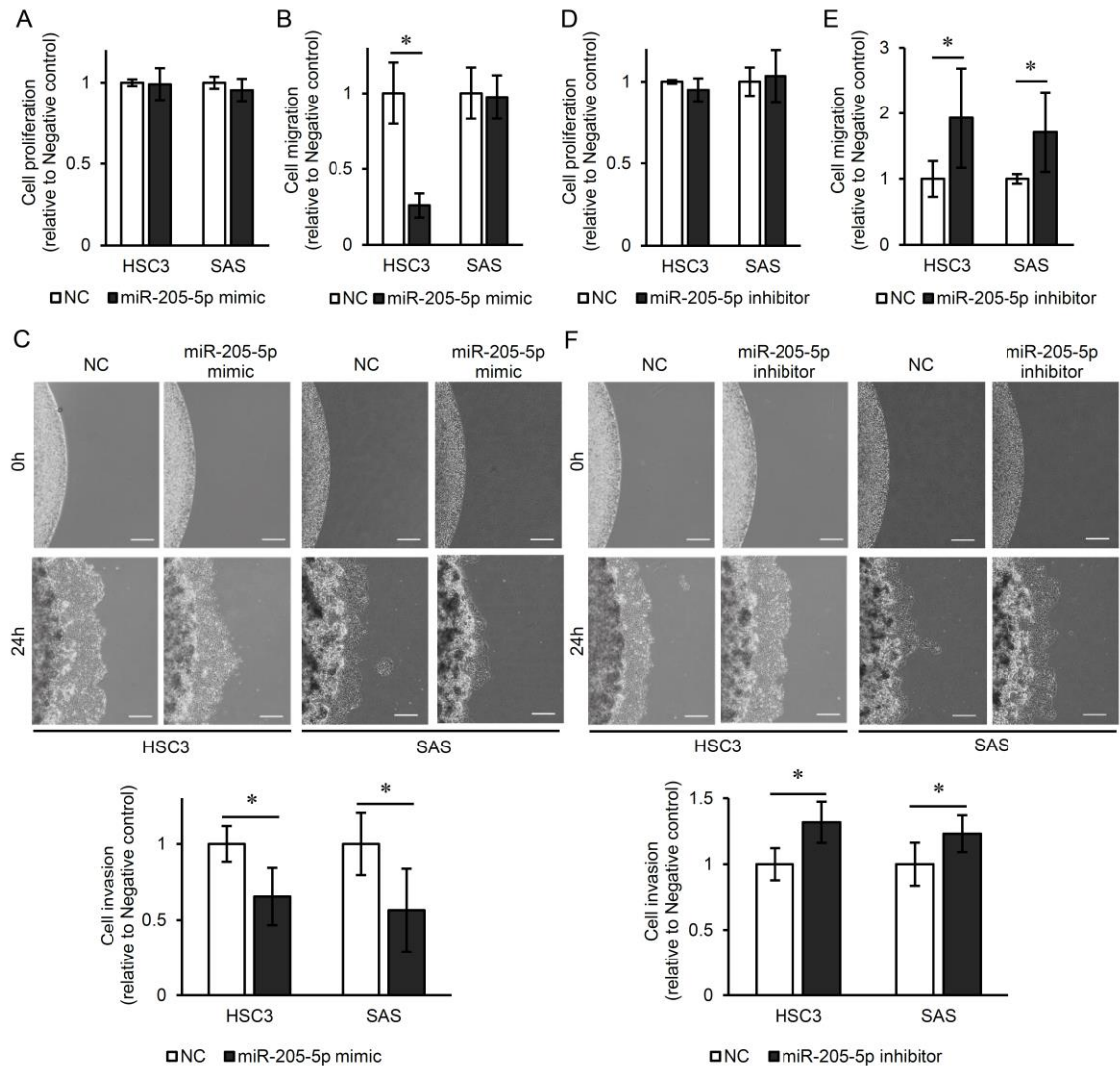


Figure 2. Effect of miR-205-5p mimic or inhibitor on OSCC-cell proliferation, migration, and invasiveness. HSC3 and SAS cells were transfected with 50 nM miR-205-5p mimic or inhibitor or a negative control. (A, D) Cells were cultured for 24 h after transfection, and then assayed for proliferation. The value for the negative control (NC) was set to 1; bars represent the average of 6 wells per treatment. Error bars are SD. (* $P < 0.05$). (B, E) Cells were cultured for 48 h after transfection and then assayed for migration. The value for negative NC was set to 1; bars represent the average of 6 wells per treatment. Error bars are SD. (* $P < 0.05$). (C, F) Cells were cultured for 48 h after transfection and then assayed for invasive activity as described in Material and Methods. The value for NC was set to 1; bars represent the average of 6 wells per treatment, and error bars are SD. (* $P < 0.05$). Scale bar in photographs: 500 μ m.

Figure. 3

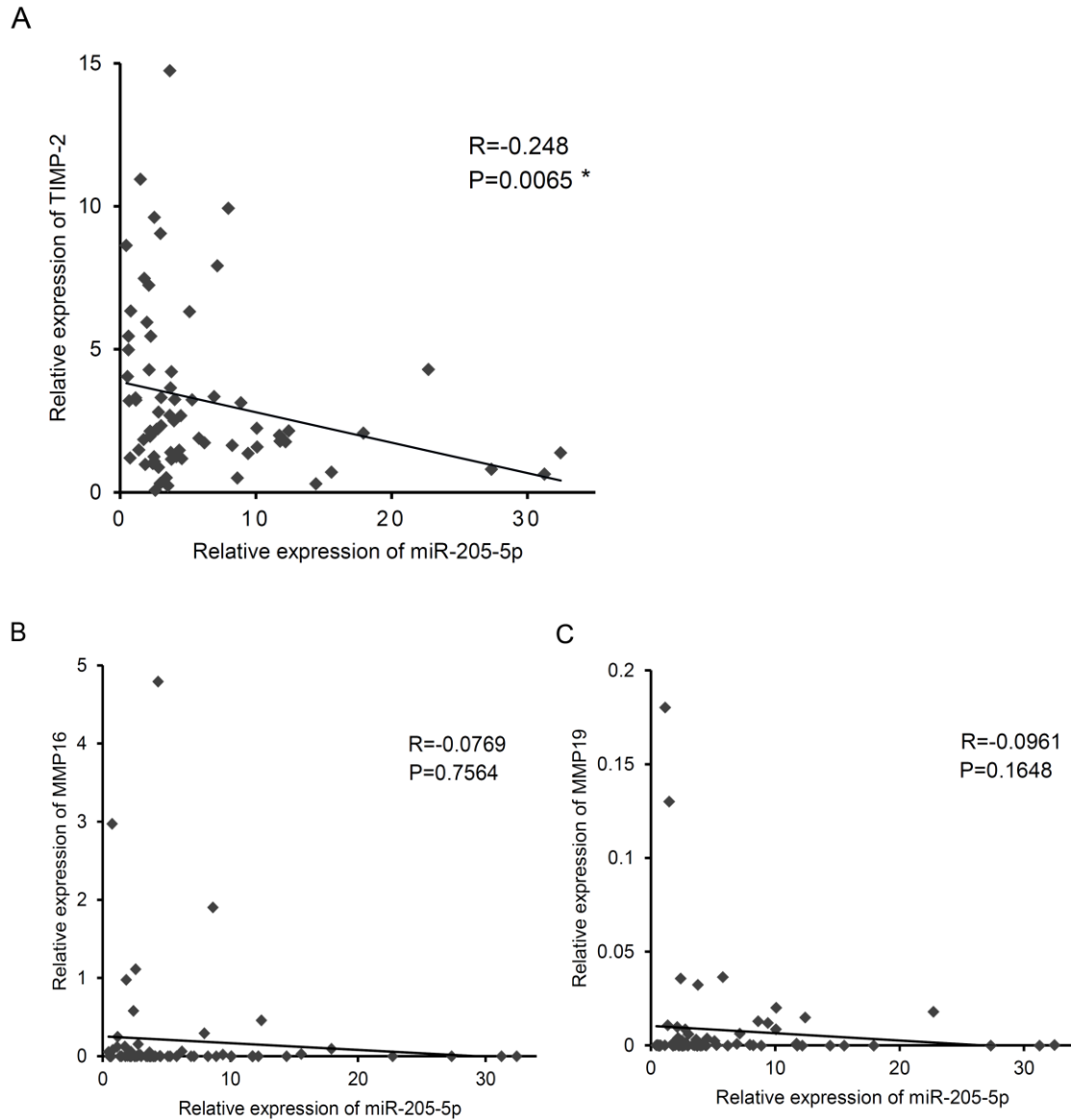


Figure 3. Negative correlation between miR-205-5p and TIMP-2 mRNA expression in OSCC specimens. (A, B, C) TIMP-2, MMP-16, MMP-19 and miR-205-5p expressions were analyzed by qRT-PCR as described in Material and Methods. TIMP-2 / MMP-16 / MMP-19 and miR-205-5p were normalized to GAPDH and RNU6B, respectively. P and R values were calculated using a Spearman's correlation test. (* $P < 0.01$)

Figure. 4

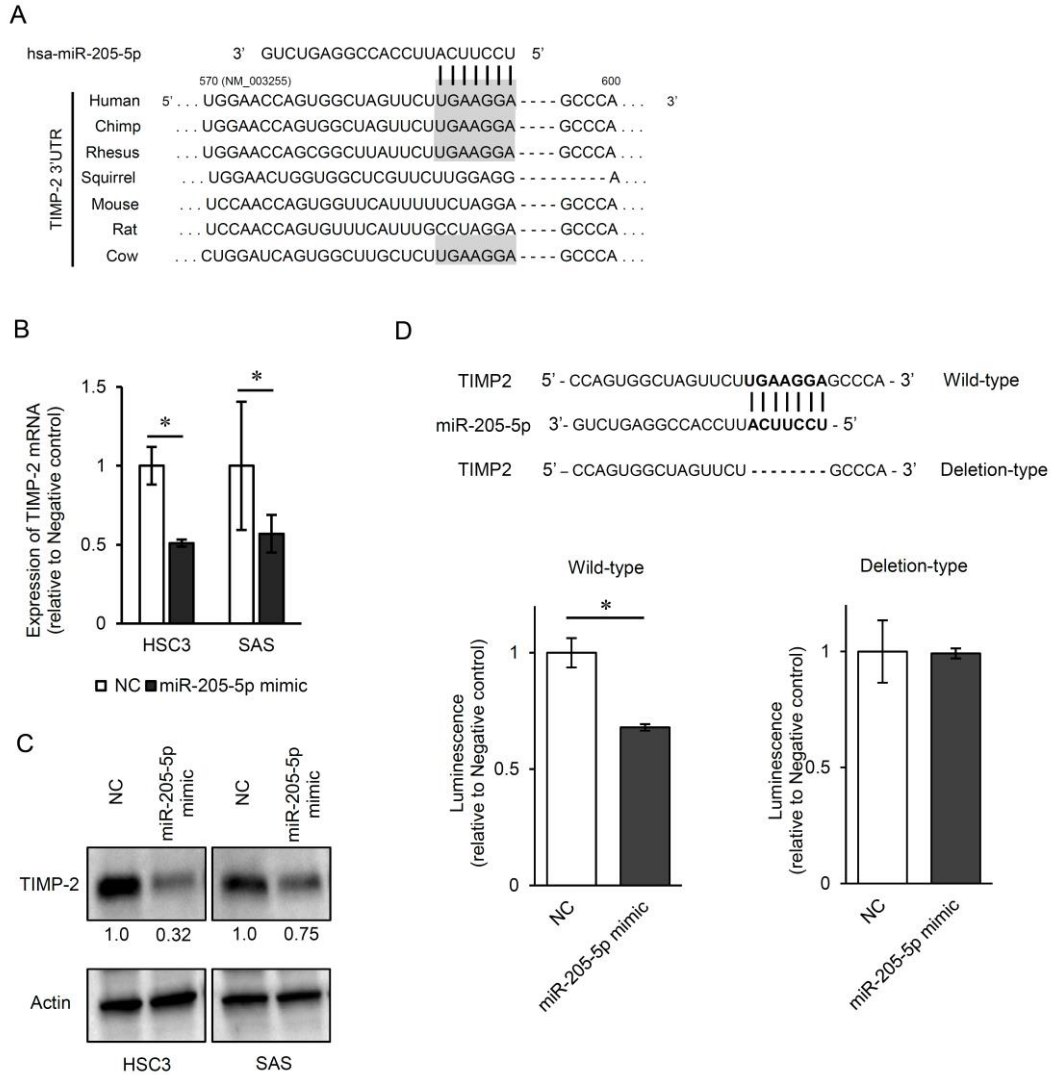


Figure 4. TIMP-2 is a direct target of miR-205-5p. (A) Schematic showing the conservation of a putative miR-205-5p target site in the 3' UTR of TIMP-2. (B) TIMP-2 mRNA levels in HSC3 and SAS cells transfected with miR-205-5p mimic or negative control. TIMP-2 was normalized to GAPDH. The expression of the negative control (NC) was set to 1; bars represent the average of 6 wells per treatment, and the error bars are SD. (*P < 0.05). (C) Western blot showing the TIMP-2 levels in HSC3 and SAS cells transfected with miR-205-5p mimic or negative control. Actin was used as a loading control. (D) Luciferase reporter assays were performed using vectors that included (Wild type) or lacked (Deletion type) the wild type sequences of the putative miR-205-5p target site. Renilla luciferase assays were normalized to firefly luciferase values. The luminescence for NC was set to 1; bars represent the average of 6 wells per treatment, and error bars are SD. (*P < 0.05).

Figure. 5

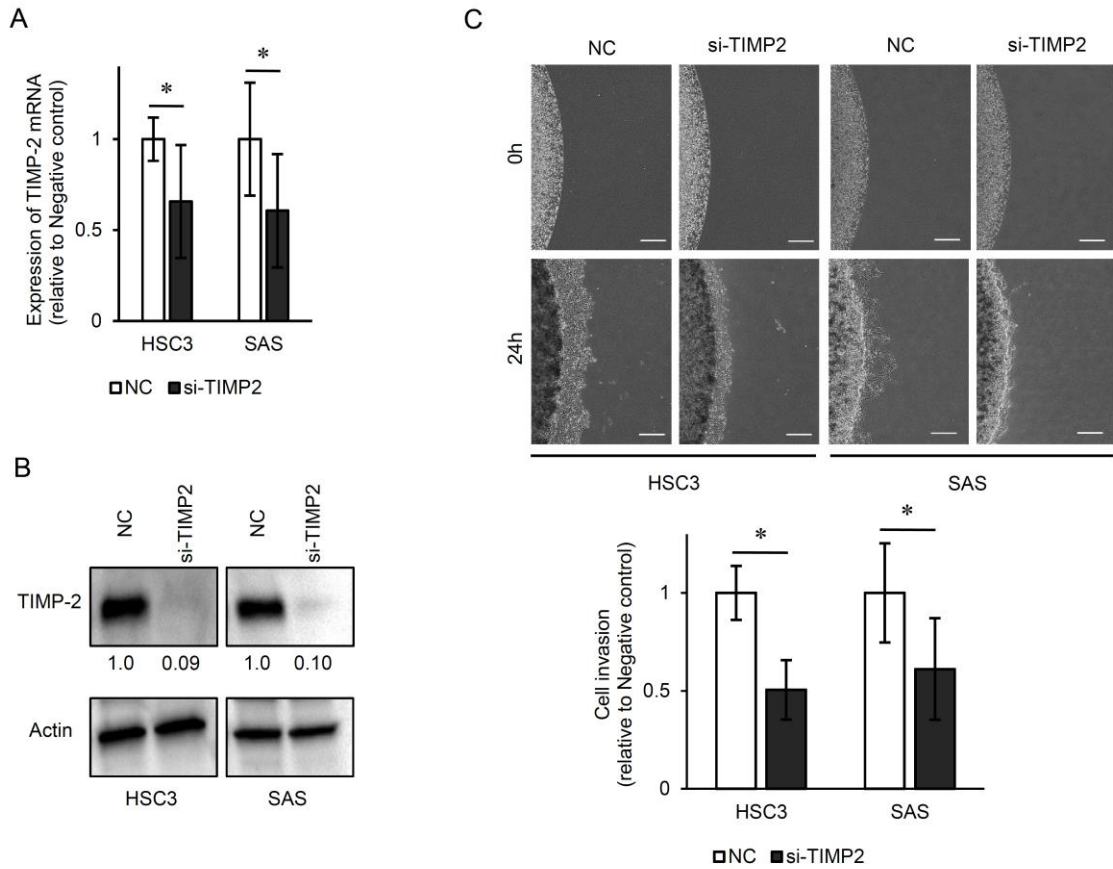


Figure 5. Effect of si-TIMP-2 transfection on OSCC cell lines. (A) TIMP-2 mRNA levels, normalized to GAPDH, in HSC3 and SAS cells transfected with si-TIMP-2 (25 nM) or negative control. The value for the negative control (NC) was set to 1; bars represent the average of 6 wells per treatment, and error bars are SD. (* $P < 0.05$). (B) Western blot showing the TIMP-2 levels in HSC3 and SAS cells after transfection with si-TIMP-2 or negative control. Actin was used as a loading control. (C) Cells were cultured for 48 h after transfection, and then assayed for invasiveness (see Material and Methods). The value for the negative control was set to 1; bars represent the average of 6 wells per treatment, and error bars are SD. (* $P < 0.05$). Scale bars = 500 μ m.

Figure. 6

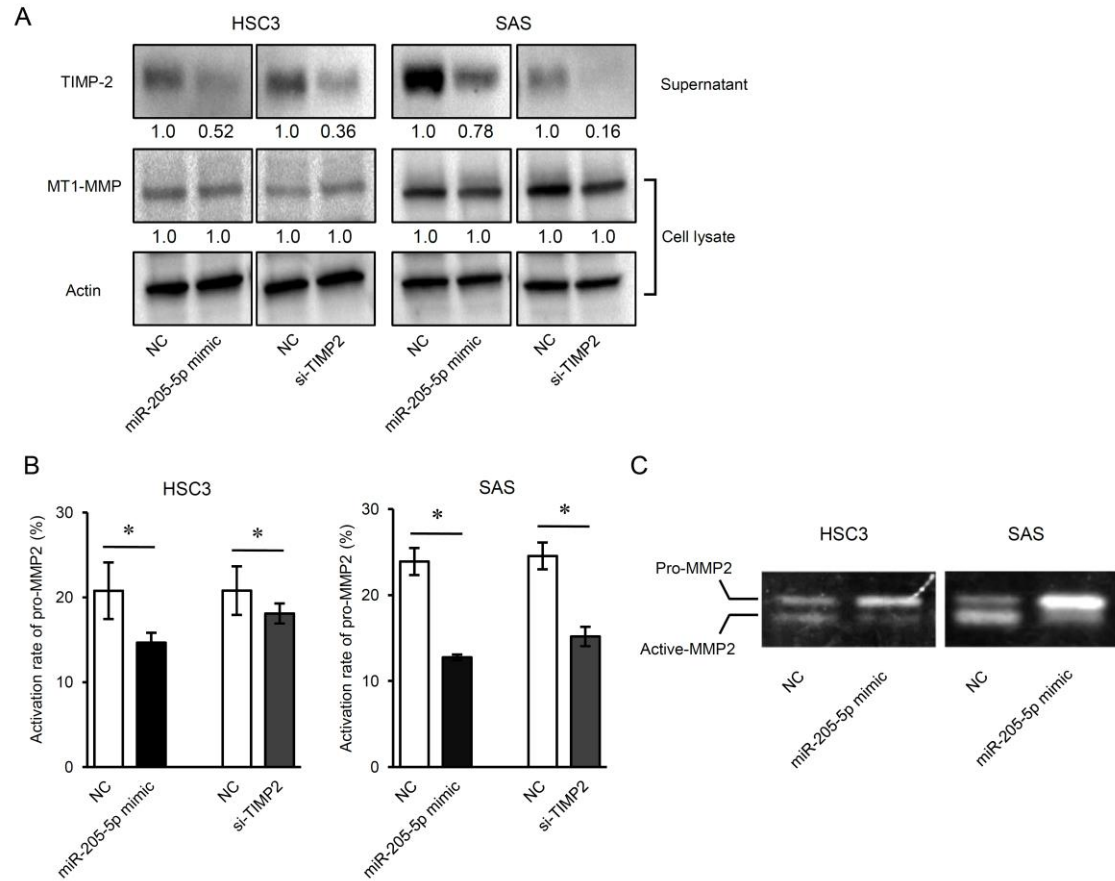


Figure 6. TIMP-2 suppression in OSCC cells reduces the activation of pro-MMP2 by the TIMP-2/MT1-MMP complex. HAC3 and SAS cells were transfected with miR-205-5p mimic, si-TIMP-2, or negative control. (A) Cells were cultured in FBS-free medium for 48 h, then the content of TIMP-2 in the culture supernatant and of MT1-MMP in the cells were analyzed by western blot. Actin was used as a loading control. (B) Cells were cultured in FBS-free medium for 48 h, and then the amount of activated pro-MMP2 in the supernatant was analyzed as described in Material and Methods. The value for negative control (NC) was set to 1; bars represent the average of 4 wells per treatment, and error bars are SD. (* $P < 0.05$). (C) Cells were cultured in FBS-free medium for 48 h, and then the MMP2 enzyme activity in the supernatant was analyzed by gelatin zymography.

Figure. 7

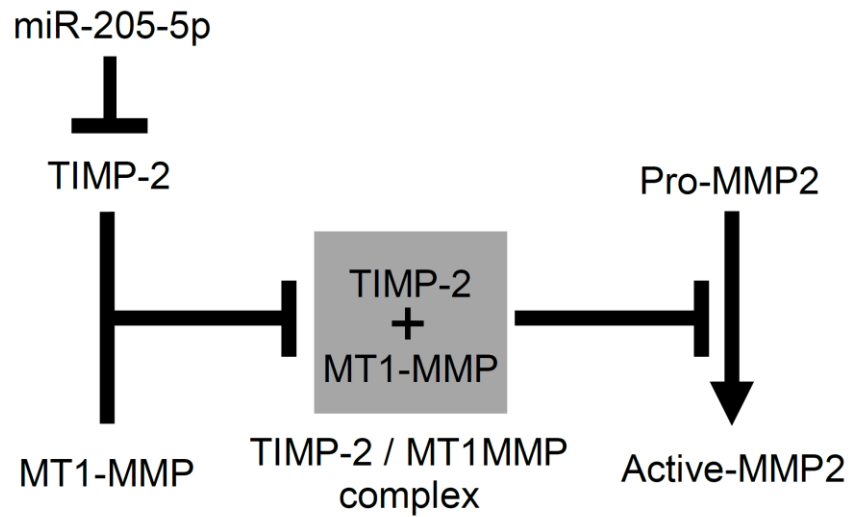


Figure 7. Pathway by which miR-205-5p regulates TIMP-2 to suppress pro-MMP-2 activation. MiR-205-5p suppresses TIMP-2 expression, reducing the amount of TIMP-2/MT1-MMP complex on the cell membrane. Thus, pro-MMP-2 activation mediated by the membrane-bound TIMP-2/MT1-MMP complex is suppressed.

References

1. Bhattacharya A, Roy R, Snijders AM, et al.: Two distinct routes to oral cancer differing in genome instability and risk for cervical node metastasis. *Clinical cancer research : an official journal of the American Association for Cancer Research* 17: 7024-7034, 2011.
2. Ferlito A, Rinaldo A, Robbins KT, et al.: Changing concepts in the surgical management of the cervical node metastasis. *Oral Oncol* 39: 429-435, 2003.
3. Greenberg JS, El Naggar AK, Mo V, Roberts D and Myers JN: Disparity in pathologic and clinical lymph node staging in oral tongue carcinoma. Implication for therapeutic decision making. *Cancer* 98: 508-515, 2003.
4. Shingaki S, Takada M, Sasai K, et al.: Impact of lymph node metastasis on the pattern of failure and survival in oral carcinomas. *American journal of surgery* 185: 278-284, 2003.
5. Woolgar JA, Rogers SN, Lowe D, Brown JS and Vaughan ED: Cervical lymph node metastasis in oral cancer: the importance of even microscopic extracapsular spread. *Oral Oncol* 39: 130-137, 2003.
6. Wikner J, Grobe A, Pantel K and Riethdorf S: Squamous cell carcinoma of the oral cavity and circulating tumour cells. *World journal of clinical oncology* 5: 114-124, 2014.
7. Bhuvarahamurthy V, Kristiansen GO, Johannsen M, et al.: In situ gene expression and localization of metalloproteinases MMP1, MMP2, MMP3, MMP9, and their inhibitors TIMP1 and TIMP2 in human renal cell carcinoma. *Oncology reports* 15: 1379-1384, 2006.
8. Kusakawa J, Sasaguri Y, Shima I, Kameyama T and Morimatsu M: Expression of matrix metalloproteinase-2 related to lymph node metastasis of oral squamous cell carcinoma. A clinicopathologic study. *American journal of clinical pathology* 99: 18-23, 1993.
9. Imai K, Ohuchi E, Aoki T, et al.: Membrane-type matrix metalloproteinase 1 is a gelatinolytic enzyme and is secreted in a complex with tissue inhibitor of metalloproteinases 2. *Cancer Res* 56: 2707-2710, 1996.
10. Strongin AY, Collier I, Bannikov G, Marmer BL, Grant GA and Goldberg GI: Mechanism of cell surface activation of 72-kDa type IV collagenase. Isolation of the activated form of the membrane metalloprotease. *The Journal of biological chemistry* 270: 5331-5338, 1995.
11. Brodersen P and Voinnet O: Revisiting the principles of microRNA target recognition and mode of action. *Nature reviews. Molecular cell biology* 10: 141-148, 2009.

12. Fukumoto I, Koshizuka K, Hanazawa T, et al.: The tumor-suppressive microRNA-23b/27b cluster regulates the MET oncogene in oral squamous cell carcinoma. *International journal of oncology* 49: 1119-1129, 2016.
13. Fukumoto I, Hanazawa T, Kinoshita T, et al.: MicroRNA expression signature of oral squamous cell carcinoma: functional role of microRNA-26a/b in the modulation of novel cancer pathways. *British journal of cancer* 112: 891-900, 2015.
14. Baba O, Hasegawa S, Nagai H, et al.: MicroRNA-155-5p is associated with oral squamous cell carcinoma metastasis and poor prognosis. *Journal of oral pathology & medicine : official publication of the International Association of Oral Pathologists and the American Academy of Oral Pathology* 45: 248-255, 2016.
15. He S, Lai R, Chen D, et al.: Downregulation of miR-221 Inhibits Cell Migration and Invasion through Targeting Methyl-CpG Binding Domain Protein 2 in Human Oral Squamous Cell Carcinoma Cells. *BioMed research international* 2015: 751672, 2015.
16. Elgamal OA, Park JK, Gusev Y, et al.: Tumor suppressive function of mir-205 in breast cancer is linked to HMGB3 regulation. *PloS one* 8: e76402, 2013.
17. Iorio MV, Casalini P, Piovan C, et al.: microRNA-205 regulates HER3 in human breast cancer. *Cancer Res* 69: 2195-2200, 2009.
18. Majid S, Dar AA, Saini S, et al.: MicroRNA-205-directed transcriptional activation of tumor suppressor genes in prostate cancer. *Cancer* 116: 5637-5649, 2010.
19. Matsushima K, Isomoto H, Yamaguchi N, et al.: MiRNA-205 modulates cellular invasion and migration via regulating zinc finger E-box binding homeobox 2 expression in esophageal squamous cell carcinoma cells. *Journal of translational medicine* 9: 30, 2011.
20. Lee GY, Kenny PA, Lee EH and Bissell MJ: Three-dimensional culture models of normal and malignant breast epithelial cells. *Nature methods* 4: 359-365, 2007.
21. Sakr M, Takino T, Sabit H, Nakada M, Li Z and Sato H: miR-150-5p and miR-133a suppress glioma cell proliferation and migration through targeting membrane-type-1 matrix metalloproteinase. *Gene* 587: 155-162, 2016.
22. Nishikawa R, Goto Y, Kojima S, et al.: Tumor-suppressive microRNA-29s inhibit cancer cell migration and invasion via targeting LAMC1 in prostate cancer. *International journal of oncology* 45: 401-410, 2014.
23. Kinoshita T, Nohata N, Hanazawa T, et al.: Tumour-suppressive microRNA-29s inhibit cancer cell migration and invasion by targeting laminin-integrin signalling in head and neck squamous cell carcinoma. *British journal of cancer* 109:

2636-2645, 2013.

24. Nelson KM and Weiss GJ: MicroRNAs and cancer: past, present, and potential future. *Molecular cancer therapeutics* 7: 3655-3660, 2008.

25. Liu L, Bi N, Wu L, et al.: MicroRNA-29c functions as a tumor suppressor by targeting VEGFA in lung adenocarcinoma. *Molecular cancer* 16: 50, 2017.

26. Zhang JK, Li YS, Zhang CD and Dai DQ: Up-regulation of CRKL by microRNA-335 methylation is associated with poor prognosis in gastric cancer. *Cancer cell international* 17: 28, 2017.

27. Chen Z, Tang ZY, He Y, Liu LF, Li DJ and Chen X: miRNA-205 is a candidate tumor suppressor that targets ZEB2 in renal cell carcinoma. *Oncology research and treatment* 37: 658-664, 2014.

28. Wu H, Zhu S and Mo YY: Suppression of cell growth and invasion by miR-205 in breast cancer. *Cell Res* 19: 439-448, 2009.

29. Wang N, Li Q, Feng NH, et al.: miR-205 is frequently downregulated in prostate cancer and acts as a tumor suppressor by inhibiting tumor growth. *Asian journal of andrology* 15: 735-741, 2013.

30. Gregory PA, Bert AG, Paterson EL, et al.: The miR-200 family and miR-205 regulate epithelial to mesenchymal transition by targeting ZEB1 and SIP1. *Nat Cell Biol* 10: 593-601, 2008.

31. Yue X, Wang P, Xu J, et al.: MicroRNA-205 functions as a tumor suppressor in human glioblastoma cells by targeting VEGF-A. *Oncology reports* 27: 1200-1206, 2012.

32. Adachi R, Horiuchi S, Sakurazawa Y, Hasegawa T, Sato K and Sakamaki T: ErbB2 down-regulates microRNA-205 in breast cancer. *Biochemical and biophysical research communications* 411: 804-808, 2011.

33. Zhang H and Fan Q: MicroRNA-205 inhibits the proliferation and invasion of breast cancer by regulating AMOT expression. *Oncology reports* 34: 2163-2170, 2015.

34. Pang H and Yue X: MiR-205 serves as a prognostic factor and suppresses proliferation and invasion by targeting insulin-like growth factor receptor 1 in human cervical cancer. *Tumour biology : the journal of the International Society for Oncodevelopmental Biology and Medicine* 39: 1010428317701308, 2017.

35. Childs G, Fazzari M, Kung G, et al.: Low-level expression of microRNAs let-7d and miR-205 are prognostic markers of head and neck squamous cell carcinoma. *Am J Pathol* 174: 736-745, 2009.

36. Lewis BP, Burge CB and Bartel DP: Conserved seed pairing, often flanked by adenosines, indicates that thousands of human genes are microRNA targets. *Cell* 120: 15-20, 2005.
37. Ondruschka C, Buhtz P, Motsch C, et al.: Prognostic value of MMP-2, -9 and TIMP-1,-2 immunoreactive protein at the invasive front in advanced head and neck squamous cell carcinomas. *Pathology, research and practice* 198: 509-515, 2002.
38. Yoshizaki T, Maruyama Y, Sato H and Furukawa M: Expression of tissue inhibitor of matrix metalloproteinase-2 correlates with activation of matrix metalloproteinase-2 and predicts poor prognosis in tongue squamous cell carcinoma. *Int J Cancer* 95: 44-50, 2001.
39. Katayama A, Bandoh N, Kishibe K, et al.: Expressions of matrix metalloproteinases in early-stage oral squamous cell carcinoma as predictive indicators for tumor metastases and prognosis. *Clinical cancer research : an official journal of the American Association for Cancer Research* 10: 634-640, 2004.
40. Sato H, Takino T, Kinoshita T, et al.: Cell surface binding and activation of gelatinase A induced by expression of membrane-type-1-matrix metalloproteinase (MT1-MMP). *FEBS Lett* 385: 238-240, 1996.
41. Hernandez-Barrantes S, Toth M, Bernardo MM, et al.: Binding of active (57 kDa) membrane type 1-matrix metalloproteinase (MT1-MMP) to tissue inhibitor of metalloproteinase (TIMP)-2 regulates MT1-MMP processing and pro-MMP-2 activation. *The Journal of biological chemistry* 275: 12080-12089, 2000.
42. Bernardo MM and Fridman R: TIMP-2 (tissue inhibitor of metalloproteinase-2) regulates MMP-2 (matrix metalloproteinase-2) activity in the extracellular environment after pro-MMP-2 activation by MT1 (membrane type 1)-MMP. *The Biochemical journal* 374: 739-745, 2003.
43. Lu KV, Jong KA, Rajasekaran AK, Cloughesy TF and Mischel PS: Upregulation of tissue inhibitor of metalloproteinases (TIMP)-2 promotes matrix metalloproteinase (MMP)-2 activation and cell invasion in a human glioblastoma cell line. *Laboratory Investigation* 84: 8-20, 2003.
44. Kudo T, Takino T, Miyamori H, Thompson EW and Sato H: Substrate choice of membrane-type 1 matrix metalloproteinase is dictated by tissue inhibitor of metalloproteinase-2 levels. *Cancer science* 98: 563-568, 2007.
45. Nishida Y, Miyamori H, Thompson EW, Takino T, Endo Y and Sato H: Activation of matrix metalloproteinase-2 (MMP-2) by membrane type 1 matrix metalloproteinase through an artificial receptor for proMMP-2 generates active MMP-2.

Cancer Res 68: 9096-9104, 2008.

46. Caterina JJ, Yamada S, Caterina NC, et al.: Inactivating mutation of the mouse tissue inhibitor of metalloproteinases-2(Timp-2) gene alters proMMP-2 activation. The Journal of biological chemistry 275: 26416-26422, 2000.

47. Wang Z, Juttermann R and Soloway PD: TIMP-2 is required for efficient activation of proMMP-2 in vivo. The Journal of biological chemistry 275: 26411-26415, 2000.

48. Itoh Y, Ito A, Iwata K, Tanzawa K, Mori Y and Nagase H: Plasma membrane-bound tissue inhibitor of metalloproteinases (TIMP)-2 specifically inhibits matrix metalloproteinase 2 (gelatinase A) activated on the cell surface. The Journal of biological chemistry 273: 24360-24367, 1998.